

# Characterization of Microwave Liquefied Bamboo Residue and Its Potential Use in the Generation of Nanofibrillated Cellulosic Fiber

Jiulong Xie,<sup>†,§,⊥</sup> Chung-Yun Hse,<sup>‡</sup> Chunjie Li,<sup>§,⊥</sup> Todd F. Shupe,<sup>§</sup> Tingxing Hu,<sup>\*,†</sup> Jinqiu Qi,<sup>†</sup> and Cornelis F. De Hoop<sup>§</sup>

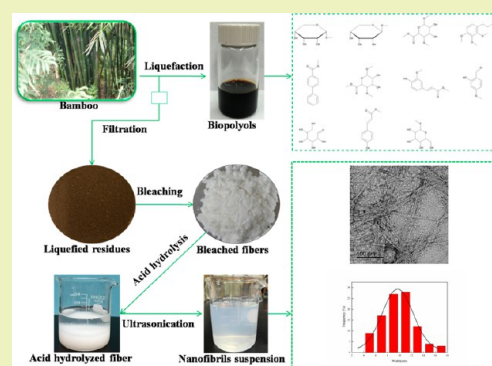
<sup>†</sup>College of Forestry, Sichuan Agricultural University, Chengdu, Sichuan 611130, China

<sup>‡</sup>Southern Research Station, USDA Forest Service, Pineville, Louisiana 71360, United States

<sup>§</sup>School of Renewable Natural Resources, Louisiana State University Agricultural Center, Baton Rouge, Louisiana 70803, United States

**ABSTRACT:** Bamboo raw feedstocks with large particle size (20–80 mesh) were subjected to a microwave liquefaction system, and the liquefied products were separated into biopolyols and liquefied residues. Biopolyols were first analyzed by gas chromatography mass spectrometry (GC–MS), and the main components were sugar derivatives with 2–4 hydroxyl groups and phenolic compounds derived from lignin. The residues were collected and evaluated for potential use in the production of nanofibrillated cellulosic fibers. Results show that liquefied residue content as well as its physicochemical properties varied with respect to particle size, liquefaction temperature, and reaction time. It was also found that residues from liquefaction reaction with the minimum residue content in this study still exhibited traced fiber structure with remaining cellulose attached with recondensed lignin. Pure white cellulose fibers were extracted from the residues with yield of 65.61% using a combination of bleaching and acid hydrolysis treatment. Nanofibrillated cellulosic fibers were generated by given the purified cellulose fibers to high-intensity ultrasonic treatment. The resulted nanofibrillated cellulosic fibers had a range of 4–18 nm in diameter and length of 550 nm or longer, indicating the nanofibers obtained from liquefied bamboo residues hold great potential in reinforcing polymeric matrix materials. The successful isolation of nanofibrillated cellulosic fibers from liquefied residues offers a novel approach to make full use of the liquefied bamboo for value-added green products.

**KEYWORDS:** Bamboo, Microwave liquefaction, Residue, Nanofibrillated cellulosic fiber, Characterization



## INTRODUCTION

Biomass is widely considered as an important feedstock because of its renewability, ease of degradation, and availability. According to Perlack and Stokes, the current biomass resource availability annually was about  $1.37 \times 10^9$  dry tons from forestlands and croplands.<sup>1</sup> Recently, utilization of biomass for bioenergy or biochemicals has attracted great attention.<sup>2–6</sup> For the production of biopolyols or biobased polymers, pyrolysis and liquefaction are two common pathways. However, liquefaction has more potential in converting biomass into valuable products because of its mild reaction conditions compared to pyrolysis.<sup>7–9</sup> Liquefaction of biomass using organic solvents under conventional heating sources, such as oil has been carried out before, and the liquefied products have been also evaluated for the preparation of polyurethane foams<sup>10,11</sup> and phenolic resins.<sup>12,13</sup>

Usually, in the conventional liquefaction system, inefficient thermal conduction on the surface of the feedstocks results in ineffective energy utilization, and very fine feedstock grinding (smaller than 200 mesh) was required because fine particles increase overall heat transfer in a certain extent. However, this

requires large amount of energy for size reduction, which in turn increases the whole energy consuming in the entire system. The application of microwave irradiation to wood liquefaction has been recently reported.<sup>14</sup> Results have shown that microwave-assisted liquefaction could convert fine grinding wood feedstock into biopolyols with a high conversion yield (>90%) in minutes.<sup>15–17</sup> This is mainly due to the fact that heating by microwave is direct and volumetric and thus results in efficient biomass conversion. Because of the benefits of microwave heating in wood liquefaction, various lignocellulosic such as wheat straw lignin,<sup>18</sup> bamboo,<sup>19,20</sup> sugarcane bagasse,<sup>21</sup> and corn stover<sup>22</sup> have been subjected to microwave-assisted liquefaction system for the production of biopolyols for alternatives of petroleum products. However, in all these studies only fine grinding feedstocks were used as raw materials, the attempts of using large particles has not been investigated.

**Received:** March 10, 2016

**Revised:** April 11, 2016

**Published:** April 17, 2016

Thus, it is worthy to examine that if microwave liquefaction could still efficiently liquefy large size feedstocks.

Even though microwave liquefaction has been recently considered as a promising approach for the conversion of renewable lignocellulosic biomass into liquid biopolymers, previous research mainly focused on the optimization of microwave liquefaction process and applications of the liquefied products on biobased materials, while the liquefied residues were discarded as waste and explorations of its potential utilizations were ignored. As for the liquefied residues, Pan et al. characterized the liquefied wood residues from different liquor ratios and cooking methods.<sup>23</sup> Zhang et al. reported the effects of the reaction time, liquefaction temperature, acid concentration, and liquor ratio on the chemical properties of the liquefied wood residues.<sup>24</sup> Results in both of these research indicated that characterization of the liquefied residues could provide information for better understanding the liquefaction behaviors of lignocellulosic biomass. The research on utilizations of liquefied lignocellulosic biomass residues has not yet been reported.

The estimated annual yield of moso bamboo was about  $1.8 \times 10^7$  tons and was greater than all other kinds of bamboo.<sup>25</sup> The integrated utilizations of moso bamboo via liquefaction may provide potential approach for the production of high-value-added bioproducts. Therefore, in this paper large particle size bamboo feedstocks were subjected to a microwave liquefaction system; the liquid products were first evaluated for further applications. Then, the remaining residue was collected and its physicochemical properties including content, morphology, and chemical structures with respect to particle size and reaction conditions were comprehensively investigated. Finally, the residues were given to chemical treatment and ultrasonic nanofibrillation process for the extraction of nanofibrillated cellulosic fibers. The specific objective of this study is aimed to elucidate the microwave liquefied bamboo residue and exploit its potential use in the production of high-value-added nanofibers. The results in this study will provide an efficient pathway in making full use of lignocellulosic biomass via microwave liquefaction and with subsequent process.

## ■ EXPERIMENTAL SECTION

**Materials and Chemicals.** Three-year-old Moso bamboo (*Phyllostachys pubescens*) was harvested in Pineville, LA, USA. Bamboo logs with length of 2 meters were cut from the middle portion of five culms were crushed into small particles using a Buffalo Hammer Laboratory Mill equipped with an 8 mm screen. Particles with size of 10–20, 20–40, 40–60, and 60–80 mesh were separated and collected by using an autoscreening machine (An RX-29 Ro-Tap). The particles were then dried to a constant weight in an oven at 105 °C. All acids, glycerol, and methanol used were of reagent grade and obtained from commercial sources.

**Microwave Liquefaction.** Liquefaction of bamboo was performed in a Milestone Ethos Ex Microwave Extraction System equipped with 100 mL Teflon vessels. A mixture of 2 g of feedstocks, 3 g of methanol, 6 g of glycerol, and 0.14 g of sulfuric acid (98%) were loaded in a vessel. For each run, four vessels were put in the oven and the maximum microwave output power was set as 550 W. The temperature was increased from room temperature to the desired temperature within 3 min and then was kept constant for 7 or 12 min. As for the microwave reaction system setup in this study, microwave power was automatically adjusted in the range of 0–550 W based on continuous feedback from the process sensors to allow the reaction to follow the desired temperature profile. For the determination of the energy requirement, the average microwave power during the whole process was calculated by taking derivative of the power curve. The

energy requirement was calculated as the average microwave power multiplied by time, and that for the reaction of 140 °C/15 min was the maximum in this study. The average microwave power for this reaction was determined to be 330 W, and the energy requirement was calculated to be  $2.97 \times 10^5$  J.

After the reaction, the vessels were cooled for approximately 30 min. At the end of the reaction, the material was dissolved in 150 mL of methanol under constant stirring for 4 h. The liquefied solutions were then vacuum-filtered through Whatman No. 4 filter paper. The solid bamboo residue retained on the filter paper was oven-dried at 105 °C and the residue yield was the mass percentage of the residue to the original weight of bamboo. For each reaction, four repeated runs were conducted; the average value as well as the standard deviation was presented.

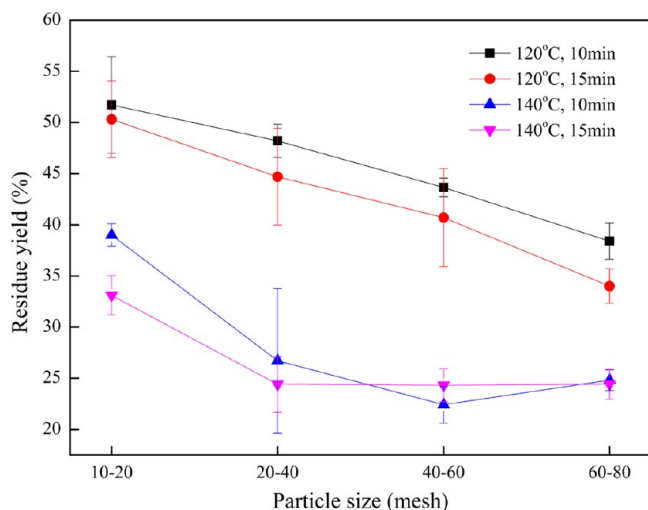
**Extraction of Nanofibrillated Cellulosic Fiber.** The residue samples were initially bleached in acidified NaClO<sub>2</sub> solution (0.1% w/v) at 75 °C for 1 h. The bleaching process was to remove the phenolic compounds or molecules from lignin retained in the fibers as well as the carbonyl groups and carboxyl groups that may be introduced during the liquefaction process. The bleaching was carried out at a 100 mL/g solution to residues. The residue was filtered and washed with deionized water until its pH was neutral. Next, 1 g of the bleached samples was hydrolyzed in 20 mL of sulfuric acid hydrolysis (2%, 25%, and 45%) at room temperature for 1 h. Hydrolysis was terminated with 10-fold cold water. The diluted suspension was vacuum-filtered. The filtered residues were rinsed with deionized water followed by centrifugation (7500 rpm at 4 °C for 15 min). The process was repeated until the pH of the precipitate was constant. The acid hydrolysis was used to eliminate traces of noncellulosic impurities and partially hydrolyzed the amorphous cellulose. The chemically purified residue samples were soaked in deionized water (concentration 0.2 wt %) and then subjected to ultrasonic fibrillation using an ultrasonic generator. The process was performed at a frequency of 25 kHz with an output power of 750 W for 25 min. The ultrasonic fibrillation was conducted in an ice bath, and the ice was maintained throughout the entire process. The sonicated suspension was centrifuged at 10000 rpm for 15 min. The precipitate was oven-dried and weighed. The weight of the nanofibrillated cellulosic fibers was the difference between the acid hydrolyzed fiber and the precipitate which was mainly composed of micro-sized and sub-micro-sized cellulosic fibers. The yield of the nanofibrillated cellulosic fiber was defined as the percentage of its weight of that of the initially charged liquefied residues.

**Characteristics Analysis.** Scanning electron microscopy (SEM) was conducted using a NeoScope (JCM-5000) scanning electron microscope to characterize the structure of the residues. All samples were attached onto the SEM stubs using carbon tabs and then coated with gold using a sputter coater (EMITECH K550X). The dimensions of the liquefied residues were measured by using a Leica laboratory micro system. The samples were pressed from two slides glass after blending with a 1:1 w/w solution of glycerol and methanol. 300 particles were randomly chosen to analyze. Analysis of variance (ANOVA) was performed to determine significant difference ( $\alpha = 0.05$ ) in residue dimensions among samples from different reactions, and the analysis was carried out using SAS (version 9.1, SAS Institute, Cary, NC). Fourier transform infrared spectroscopy (FT-IR) analysis of the samples was performed by a Nicolet Nexus 670 spectrometer equipped with a Thermo Nicolet Golden Gate MKII Single Reflection ATR accessory. A small amount of residue was applied directly on the diamond crystal. Data collection was performed with a  $4 \text{ cm}^{-1}$  spectral resolution and 32 scans were taken per sample. Lignin content of bamboo raw material and the liquefied residue samples was determined in accordance to a referenced method.<sup>26</sup> Three repetitions were conducted for each sample. Nanofibrillated cellulosic fibers were confirmed by transmission electron microscopy (TEM). The concentration of aqueous nanofibers suspensions was diluted from 0.2% to 0.01% (w/w). A droplet of the diluted suspension was deposited on the surface of carbon-coated copper grids. As for contrast in TEM, the nanofibers were negatively stained in a 2% (wt) solution of uranyl acetate. The morphology of the nanofiber was observed using

a transmission electron microscope (TEM, JEOL 100CX, JEOL, Inc., Peabody, MA, USA) with an accelerating voltage of 80 kV. The diameter of the nanofibrils was calculated by measuring 100 fibers randomly selected from several TEM images.

## RESULTS AND DISCUSSION

**Microwave Liquefaction of Bamboo.** The residue content with respect to particle size and different reaction conditions are shown in Figure 1. With reaction conditions of



Note: Error bars represent the standard deviations

**Figure 1.** Residue content with respect to bamboo particle size under various liquefaction conditions.

120 °C/10–15 min, the residue yield decreased with decreasing particle size. As for particle size, it is generally considered that the smaller the size or volume of the particle, the larger the surface area of the particle. From the results in this study,

particles of smaller size could be more easily attacked or accessed by chemicals resulting in a uniform distribution of feeding materials in the dispersion. Meanwhile, microwave energy penetrates and produces a volumetrically distributed heat source; heat is generated throughout the material and leads to faster heating rates.<sup>17</sup> Therefore, the uniform distribution of chemical reagents in smaller particles combined with the uniformly distributed heat induced by microwave energy enhanced the decomposition of bamboo, which resulted in relative low residue content.

For comparison, the residue content from 120 °C/15 min was lower than that from 120 °C/10 min, revealing that prolonging the reaction time could accelerate the liquefaction extent of bamboo.

With the reaction temperature of 140 °C, the residue content with respect to particle size exhibited a different pattern compared to that at 120 °C; i.e., the residue content first decreased and then stayed stable, indicating that recondensation occurred in the liquefaction of bamboo with a smaller particle size (proved by the higher lignin content as discussed latter). This result demonstrated that smaller particles could not only enhance the decomposition with mild reaction conditions (120 °C) but could also contribute to the repolymerization by a critical liquefaction process (liquefaction under higher temperature with longer reaction time).

Chemical compositions of the biopolyols from the liquefaction conditions of 140 °C, 15 min, 60–80 mesh were analyzed using GC–MS. The GC–MS chromatogram and structures of the identified components in the biopolyols is presented in Figure 2. The majority of compounds decomposed from bamboo were composed of five carbon sugars (alpha. -Ribopyranoside, methyl; beta. -D-Ribopyranoside, methyl), six carbon sugars [A-allose; alpha. -D-glucopyranoside, methyl; methyl (methyl 4-O-methyl-. alpha. -D-mannopyranoside)-urate], and phenolic compounds [3-(2,3,4-trimethoxyphenyl)propionic acid; 2-propenoic acid, 3-(4-

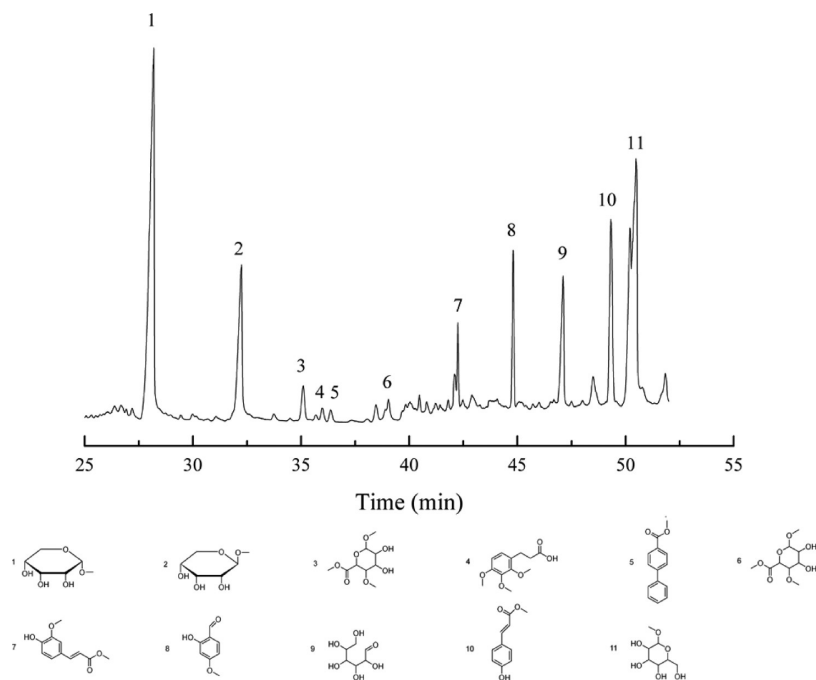


**Figure 2.** GC–MS chromatograms and chemical structures of compositions of the biopolyols from microwave liquefied bamboo particles (60–80 mesh) at 140 °C within 15 min.

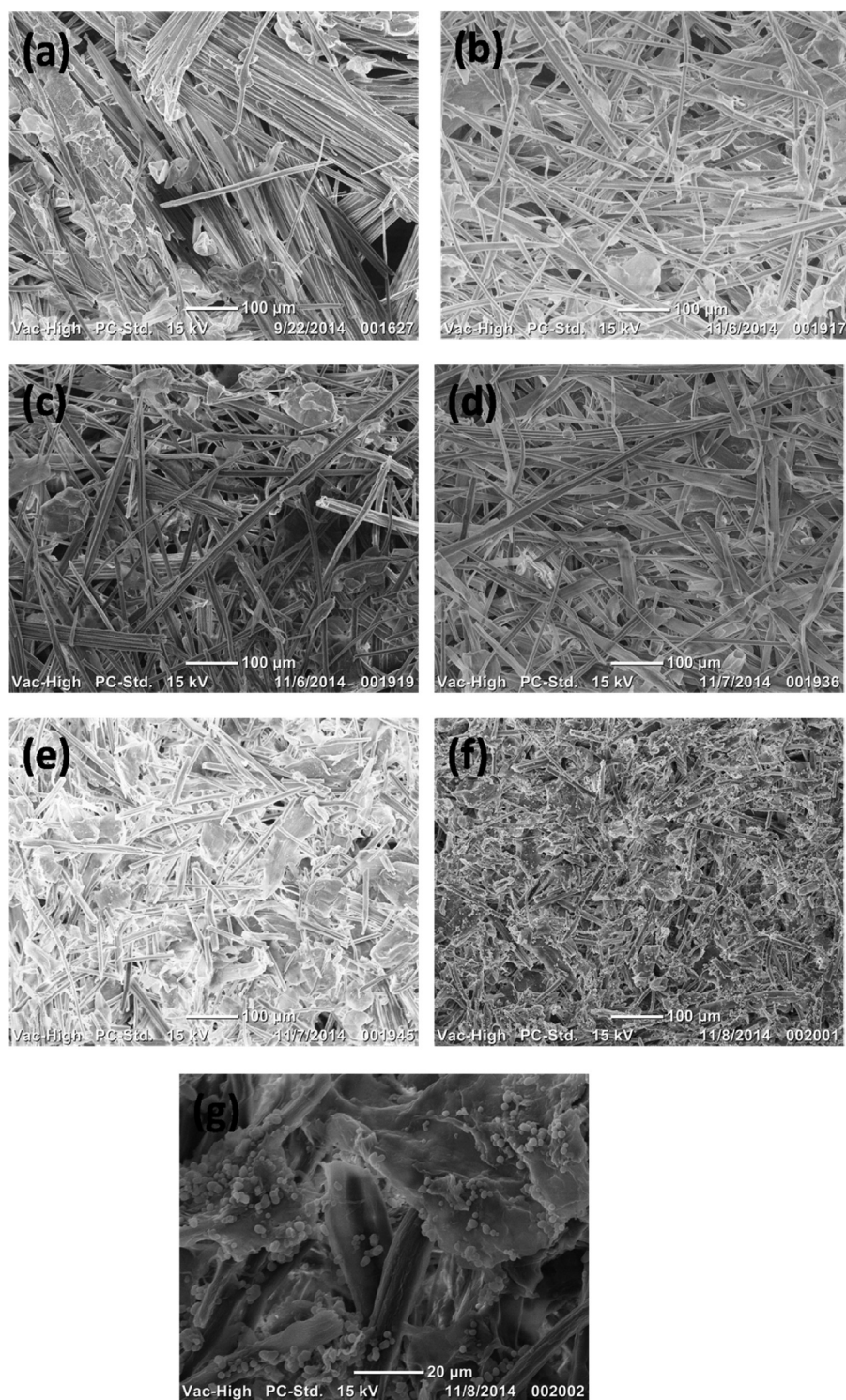


**Figure 3.** SEM images of liquefied residues obtained from different reaction conditions: (a) 120 °C, 10–20 mesh, 10 min; (b) 120 °C, 20–40 mesh, 10 min; (c) 120 °C, 60–80 mesh, 10 min; (d) 140 °C, 10–20 mesh, 10 min; (e) 140 °C, 10–20 mesh, 15 min; (f) 140 °C, 60–80 mesh, 10 min, 150 $\times$ ; (g) 140 °C, 60–80 mesh, 10 min, 800 $\times$ . Other conditions: glycerol/methanol, 2/1; microwave power, 550 W; sulfuric acid, 1.75%; solvent/bamboo, 4.5/1.

hydroxyphenyl)-, methyl ester; benzaldehyde, 2-hydroxy-4-methoxy-; methyl biphenyl-4-carboxylate]. The presence of C<sub>5</sub> and C<sub>6</sub> sugars derived from hemicellulose and cellulose indicated the degradation of carbohydrates, and the aromatics in the biopolyols evidenced the decomposition of the lignin. Because the sugar derivatives processed 2–5 hydroxyl groups, the biopolyols in this study could be used as potential chemicals

for the preparation of polyurethane foams because of its large amount of hydrogen bonds. Further analysis and potential utilizations of the biopolyols will be evaluated in another study.

**Morphology Analysis of Liquefied Residues.** The microstructures of the liquefied bamboo residues were characterized by SEM, and the SEM images are presented in Figure 3. The images showed that the liquefied bamboo

Table 1. Changes in Dimensions of the Liquefied Residues under Various Conditions

samples	length			diameter			aspect ratio		
	before liquefaction ( $\mu\text{m}$ )	after liquefaction ( $\mu\text{m}$ )	reduction (%)	before liquefaction ( $\mu\text{m}$ )	after liquefaction ( $\mu\text{m}$ )	reduction (%)	before liquefaction ( $\mu\text{m}$ )	after liquefaction ( $\mu\text{m}$ )	increment (%)
120 10 min									
10–20 mesh	7164	1063	85.16	1056	15	98.58	8	71	787.5
20–40 mesh	7166	1015	85.84	477	11	97.69	17	92	441.18
40–60 mesh	3449	679	80.31	233	11	95.28	17	62	164.71
60–80 mesh	1008	385	61.81	113	11	90.27	11	35	218.18
120 15 min									
10–20 mesh	7164	880	87.72	1056	13	98.77	8	68	750
20–40 mesh	7166	954	86.69	477	11	97.69	17	87	411.76
40–60 mesh	3449	657	80.95	233	10	95.71	17	66	288.24
60–80 mesh	1008	378	62.5	113	10	91.15	11	38	245.45
140 10 min									
10–20 mesh	7164	594	91.71	1056	12	98.86	8	50	525
20–40 mesh	7166	459	93.59	477	11	97.69	17	42	147.06
40–60 mesh	3449	238	93.1	233	11	95.28	17	22	29.41
60–80 mesh	1008	281	72.12	113	12	89.38	11	23	109.09
140 15 min									
10–20 mesh	7164	580	91.9	1056	11	98.96	8	53	562.5
20–40 mesh	7166	159	97.78	477	9	98.11	17	18	5.88
40–60 mesh	3449	152	95.59	233	9	96.14	17	17	0
60–80 mesh	1008	137	86.31	113	10	91.15	11	14	27.27

residues exhibited microsized shape and composed of fibers and parenchymas. Residues mainly consisted of long fibers and fiber bundles were obtained from liquefaction of 120 °C/20–40 mesh/10 min (Figure 3a), whereas the residues with short fibers and flat cell fragments were observed on the image for samples from 120 °C/60–80 mesh/10 min (Figure 3c). This result indicated that bamboo tissues were much more easily susceptible to decomposition as the particle size decreased with microwave liquefaction. It is known that the middle lamella possesses the most lignin, and then the cell wall itself.<sup>27</sup> Because single fibers and parenchymas were shown in the residues from reactions of 120 °C, it could be concluded that lignins in the middle lamella should be all dissolved and resulting in the dissociation of bamboo fiber bundles.

Figure 3 also illustrates the effect of temperature on the morphology of the residues. For comparison, residues from conditions of 140 °C/10–20 mesh/10 min were found to have much less complete fibers than those from 120 °C/10–20 mesh/10 min. Most of the residues from 140 °C were broken cells (fibers and parenchymas) (Figure 3d,e). It is apparent that the cell wall components have been decomposed under 140 °C. As for the cell wall, its dominate component is microfibrils (aggregated by cellulose molecules) embedded in matrix polymers such as lignin and hemicellulose.<sup>28</sup> The damage of the cell wall indicated that lignin and hemicellulose wrapped around the microfibrils has been almost completely decom-

posed and the exposure of the microfibrils to the chemical reagents resulted in the depolymerization of celluloses. The changes in microstructures of residues with respect to reaction conditions may also provide explanation that the liquefaction of bamboo components was in the order of lignin, hemicellulose, and then cellulose. Significant differences in residue morphology between samples from 140 °C/10 min (Figure 3d) and 140 °C/15 min (Figure 3e) were also found, revealing that at 140 °C reaction time could significantly affect the microstructures of the residues. It was interesting to note that small spherical granule substances were observed on the surface of residues from 140 °C/60–80 mesh/15 min (Figure 3f). The observed granules were ascribed to recondensed lignin fragments.<sup>29</sup> This result revealed that microwave liquefaction of bamboo particles under 140 °C was complicated involving decomposition and recondensation.

To clarify further the changes in morphology of the liquefied bamboo residues during microwave liquefaction, dimensions including length, diameter, and aspect ratio of the residues were measured. The dimensions of the residues with respect to particle size from different liquefaction temperatures (120/140 °C) are shown in Table 1. The result in Table 1 shows that liquefaction temperature has a significant effect on the length of the residue, i.e., the length of residue was significantly reduced (56.75%) when the reaction temperature increased from 120 to 140 °C. However, no significant changes in residue diameter

were observed with an increase in the reaction temperature. This result allowed the statement that liquefaction of bamboo using microwave energy primarily caused the reduction of bamboo particles along the longitudinal direction. This finding is consistent with the fact that no ray cells/units exist in the radial direction of bamboo, and the reagents primarily penetrated in the longitudinal plane, and thus reduced the fiber length. Furthermore, with the reaction processing, the aspect ratio of the residue dramatically decreased as the reaction temperature increased from 120 to 140 °C. Because there was no significant reduction in diameter, the reduction in length highly contributed the decrease of the aspect ratio.

The results in Table 1 also demonstrate the effect of particle size on particle dimensional change after liquefaction. As shown in Table 1, at 120 °C, the reduction in length slightly increased as the particle size increased, revealing that bamboo with a larger particle size could be also efficiently liquefied or dissolved. This may be due to the uniform heating by microwave energy throughout the material, and particle size had no significant effect on the liquefaction efficiency based on residue dimensions. Particle size did not affect the variation in the residue diameter because no apparent variability was observed with decreasing particle size. According to the ANOVA analysis, no significant difference in diameter was found among the residues from the liquefaction of bamboo with different sizes. At 120 °C, the increment in aspect ratio showed a decreasing trend as the particle size decreased. With the temperature ascending to 140 °C, a relative high aspect ratio can be seen in the particle size of 10–20 mesh and then the aspect ratio decreased to 14–18 as the particle size decreased (20–40 mesh to 60–80 mesh), indicating that bamboo fiber was thoroughly degraded.

**Chemical Analysis of Liquefied Residues.** FTIR spectra were used to character the chemical structure of both bamboo and liquefied residues. As shown in Figure 4, the –OH stretching vibration at 3309  $\text{cm}^{-1}$  and the methyl and methylene stretching vibration at 2881  $\text{cm}^{-1}$  in these spectra are nearly the same. The peak at 1728  $\text{cm}^{-1}$ , which was

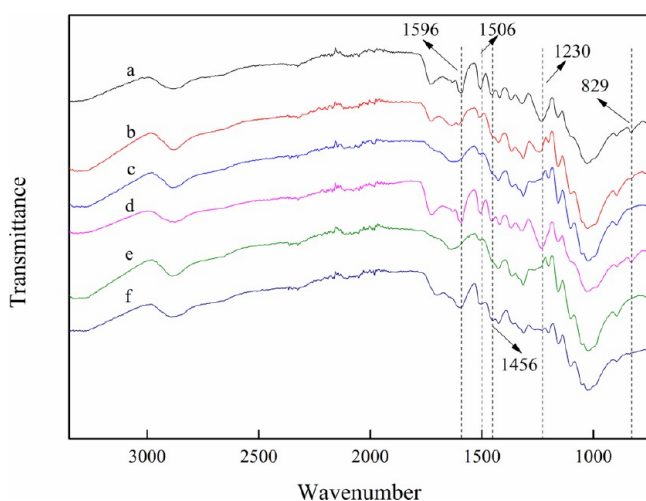


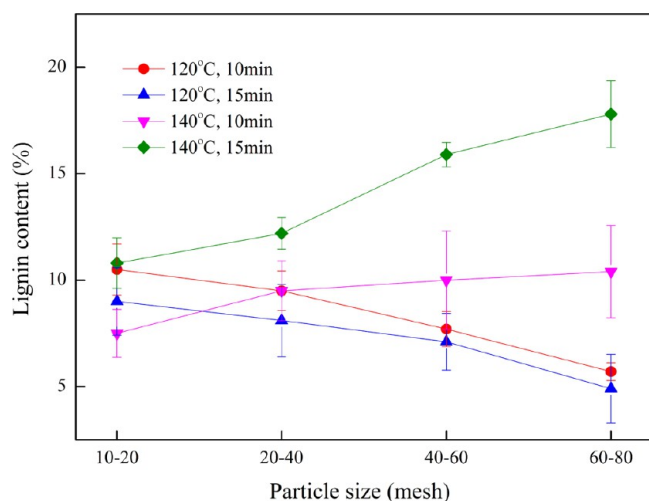
**Figure 4.** FT-IR transmittances of (a) bamboo material of 10–20 mesh; (b) 120 °C, 10–20 mesh, 15 min; (c) 140 °C, 10–20 mesh, 15 min; (d) bamboo material of 60–80 mesh, 15 min; (e) 120 °C, 60–80 mesh, 15 min; (f) 140 °C, 60–80 mesh, 15 min. Other conditions: glycerol/methanol, 2/1; microwave power, 550 W; sulfuric acid, 1.75%; solvent/bamboo, 4.5/1.

assigned to C=O stretching vibration of the carboxyl and acetyl groups in hemicellulose, had a weak tendency after liquefaction. It was almost reduced to a shoulder in the spectra of residues from 120 °C/60–80 mesh/15 min and 140 °C/10–20 mesh/15 min, indicating that hemicellulose could be easily decomposed during the liquefaction process, whereas at reaction conditions of 140 °C/60–80 mesh/15 min, intensive peak was displayed. This may be due to the recondensation of the decomposed hemicellulose derivatives in acid glycerol.

The strong absorptions at 1596, 1506, and 1456  $\text{cm}^{-1}$  in Figure 4a,d are characteristic peaks for the aromatic skeleton vibration of bamboo. Residues from 140 °C/10 min/10–20 mesh showed the lowest intensities at 1596 and 1506  $\text{cm}^{-1}$ . The peaks at 1456 and 1230  $\text{cm}^{-1}$  were related to C–H deformation combined with aromatic ring vibration and the methoxyl groups of lignin. The two groups have more intense peaks in original bamboo compared to the liquefied residues. However, the absorptions at 1596 and 1456  $\text{cm}^{-1}$  in the spectrum of residues from 140 °C/15 min/60–80 mesh intensified again, this was due to the interactions of the decomposed lignin components forming an aromatic network. This result was consistent with the higher residue yield under the liquefaction conditions and was further evidenced by the higher lignin content in the residues as discussed later. The bands at 1316, 1103, and 895  $\text{cm}^{-1}$  were all attributed to cellulose that was assigned to O–H in plane bending and CH<sub>2</sub> wagging, and glucose ring asymmetric valence vibration, respectively. The predominant peak at 1020  $\text{cm}^{-1}$  was assigned to the C–OH bending model. The insignificant changes in these cellulose bands among the spectra of bamboo and liquefied residues indicate that cellulose was the main resistance to the liquefaction system despite the variety in particle size and reaction conditions.

From the morphology and the chemical structure analysis results, the liquefied residues mainly exhibited a fiber structure with remaining cellulose. Because the liquefied residues showed a brown color, we predicted that unliquefied lignin or recondensed lignin derivatives were existed in the residues because lignins are responsible for the brown color of the liquefied residues. Therefore, the lignin content of the liquefied residues was determined, and the results are shown in Figure 5.

The lignin content for original bamboo particles was 27.31%. The lignin content slightly decreased with decreasing particle size under reaction conditions of 120 °C/10 min and 120 °C/15 min, indicating that the reduction in particle size could accelerate the decomposition of lignin. The lignin content for the residue from 120 °C/15 min/60–80 mesh was the lowest (4.9%). This result was concord with the morphology of the residues, which were composed of well displayed long fibers (Figure 3a–c). For the liquefaction at 140 °C, the lignin content for the residues from liquefaction of 10–20 mesh with 10 min was the lowest. The lignin content displayed an increase trend with decreasing particle size under reaction conditions of 140 °C/10 min and 140 °C/15 min. This result may be attributed to the self-depolymerization and/or recondensation of decomposed lignin obtained at the initial solvolysis process, and the recondensed lignin fragments, usually with large molecular weight, could not be redissolved, and thus resulted in higher lignin content in the residues.<sup>30</sup> As for the liquefaction of 10–20 mesh samples, in the initial step, reactions mainly occurred on the outer surface of the particles. With the reagents slowly permeating through the whole particles, the fluid of the reagents combined with the uniform heat source promoted the



Note: Error bars represent the standard deviations

**Figure 5.** Lignin content in microwave liquefied bamboo residues with respect to particle size under different reaction conditions.

decomposition of the cell wall components, mainly lignin. Therefore, it can be concluded that liquefaction of large particles with microwave energy resulted in the dissociation of tissue elements by dissolving lignin along with the reagent permeating process. Because particles with smaller sizes could be more easily accessed by chemicals, the degradation of cell wall components occurred immediately as the microwave radiation was introduced into the liquefaction system, which contributed to solvolysis of the overall particles. Then repolymerization of the already decomposed lignin compounds took place, resulting in higher lignin content for the residue. This coincides with the aggregated lignin granules that were observed on the surface of residues from 140 °C/60–80 mesh/15 min.

**Extraction of Nanofibrillated Cellulosic Fiber.** On the basis of the aforementioned analysis, the microwave liquefied bamboo residues were mainly composed of microfibrils attaching with noncellulosic materials, indicating that the residues had potential in the extraction of cellulose nanofibrils. To isolate nanofibrillated cellulosic fibers from the liquefied residues, residue samples from liquefaction of 120 °C/60–80 mesh/15 min and 140 °C/60–80/15 min were used and treated with chemical treatment prior to the nanofibrillation process. The steps involved during the process and visual changes of the samples in each step are illustrated in Figure 6. The dark brown color of the residues was changed to pure white after bleaching. The influence of sulfuric acid concentration used in the acid hydrolysis process and the ultrasonic treatment time on the yield of nanofibrillated cellulosic fiber were elucidated.

Table 2 presents the effect of sulfuric acid concentration on the yield of chemically purified cellulose and nanofibrillated cellulosic fiber. As the sulfuric acid concentration increased from 2% to 45%, the yield of purified cellulose decreased, whereas that of the nanofibrillated cellulosic fiber increased. Because the sulfuric acid mainly worked on the removal of noncellulosic materials and hydrolyzed the amorphous cellulose, the higher of its concentration, the more noncellulosic substances it eliminates and the higher the crystal cellulose remains; therefore, it could be easily understood that with increasing acid concentration, the yield of nanofibrillated

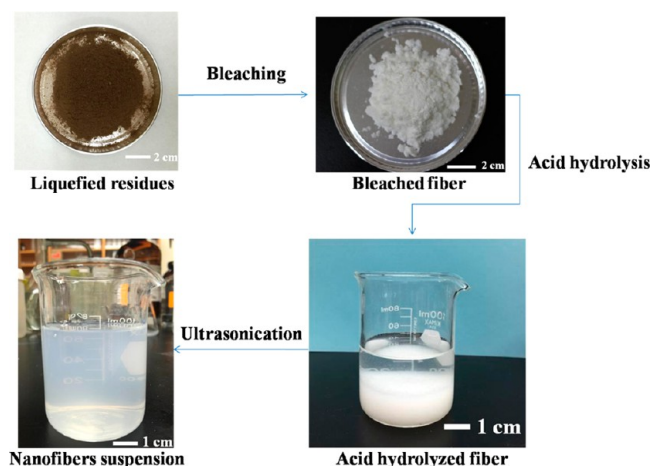


**Figure 6.** Photographs of procedures in the generation of nanofibrillated cellulosic fiber from microwave liquefied bamboo residues.

**Table 2.** Yield of Chemically Purified Cellulose Fibers and Nanofibrillated Cellulosic Fiber from Microwave Liquefied Bamboo Residues<sup>a</sup>

sample	yield of chemically purified cellulose (%)	yield of nanofibrillated cellulosic fiber (%)
120 °C/2.0%	85.60	10.75
120 °C/25%	77.78	31.96
120 °C/45%	69.59	37.18
140 °C/2.0%	78.07	37.17
140 °C/25%	67.09	50.20
140 °C/45%	65.61	52.02

<sup>a</sup>Ultrasonic time: 25 min.

cellulosic fiber increased. For comparison, residue samples from liquefaction at 140 °C yielded less purified cellulose and more nanofibrillated cellulosic fibers than those from 120 °C, respectively. At 140 °C, the cellulose in bamboo started to decompose as evidenced by the damaged cell walls shown in the SEM images because cellulose was the dominant component of the cell wall. Meanwhile, recondensation of lignin also took place at 140 °C. The degradation of the cellulose and recondensation of lignin both contributed to the relative low purity of cellulose in the residues leading to the low yield of the purified cellulose. The higher yield of nanofibrillated cellulose from residues of 140 °C may be due to that the cellulose structure was disrupted during the liquefaction and with chemical purification and ultrasonic treatments crystal nano fibrils could be easily split off resulting high nanofibrillated cellulosic fiber yield.

The effect of high-intensity ultrasonic time on the nanofibrillated cellulosic fiber yield is shown in Figure 7. It can be seen that the yield showed significant increase with increasing the ultrasonic time. This result indicated that ultrasonic time had obvious impact on nanofibrillated cellulosic fiber yield. This was because the use of ultrasonic treatment can break the hydrogen bonds and disintegrate microfibrils into nanofibrils. Though, the nanofibrillated cellulosic fiber yield isolated from different liquefied bamboo residues all showed increasing trend with respect to ultrasonic time, the yield of nanofibrillated cellulosic fibers generated from residues from liquefaction of 140 °C was always higher than those from 120 °C. This may be explained by the differences in the characteristics of the two kinds of residues.

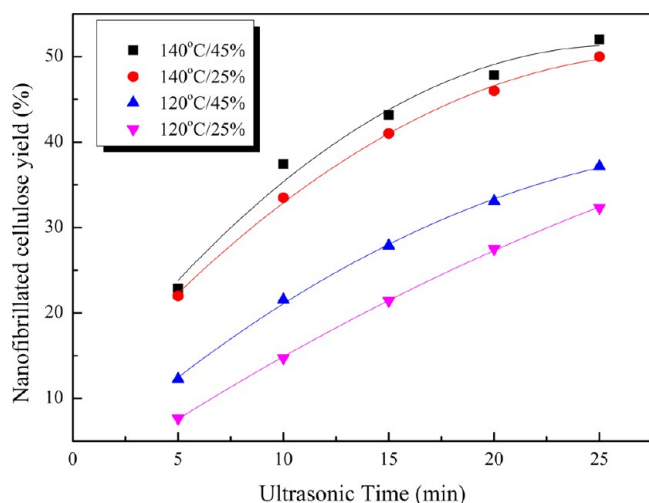


**Figure 7.** Effect of ultrasonic time on yield of nanofibrillated cellulose fiber from microwave liquefied bamboo residues.

Transmission electron microscopy (TEM) image of the nanofibrillated cellulose fibers produced from microwave liquefied bamboo residues is shown in Figure 8. The TEM images demonstrate the presence of nanofibrils. The nanofibrils had a length of 550 nm or longer and ranged roughly around 4–18 nm in diameter. Figure 8 also illustrates that liquefaction conditions, acid concentration, and ultrasonic time had no

influence on the morphology of the produced nanofibrillated cellulose fibers. In terms of nanofiber dimensions, the resulted nanofibrillated cellulose fibers had comparable properties to those isolated from raw lignocellulosic biomass as reported in other studies.<sup>31–33</sup> The results indicated that nanofibrillated cellulose fibers generated from microwave liquefied bamboo residues had potential in the fabrication of nanofiber reinforced composite materials.

## CONCLUSIONS

Biopolymers comprising C<sub>5</sub> and C<sub>6</sub> sugars and phenolic compounds were produced by microwave liquefaction of bamboo despite the large particle size. Feedstocks with smaller particles could accelerate the liquefaction with low temperature (120 °C), whereas lead to lignin recondensation under high temperature (140 °C). The chemical and morphology analysis results revealed the liquefied bamboo residues retained fiber structure and remaining cellulose. Bleaching and acid hydrolysis were proved to be efficient process in purifying the residues for pure white cellulose fibers. The chemically purified cellulose fibers from liquefied residues were reduced to nanofibrillated cellulose fibers by given to high-intensity ultrasonic treatment. Characteristics of liquefied samples, acid hydrolysis, and ultrasonic time were impact factors on the yield of nanofibrillated cellulose fibers. The generated nanofibrillated cellulose fibers were in the range of long nanofibrils, which was suitable for use in reinforcing composites.

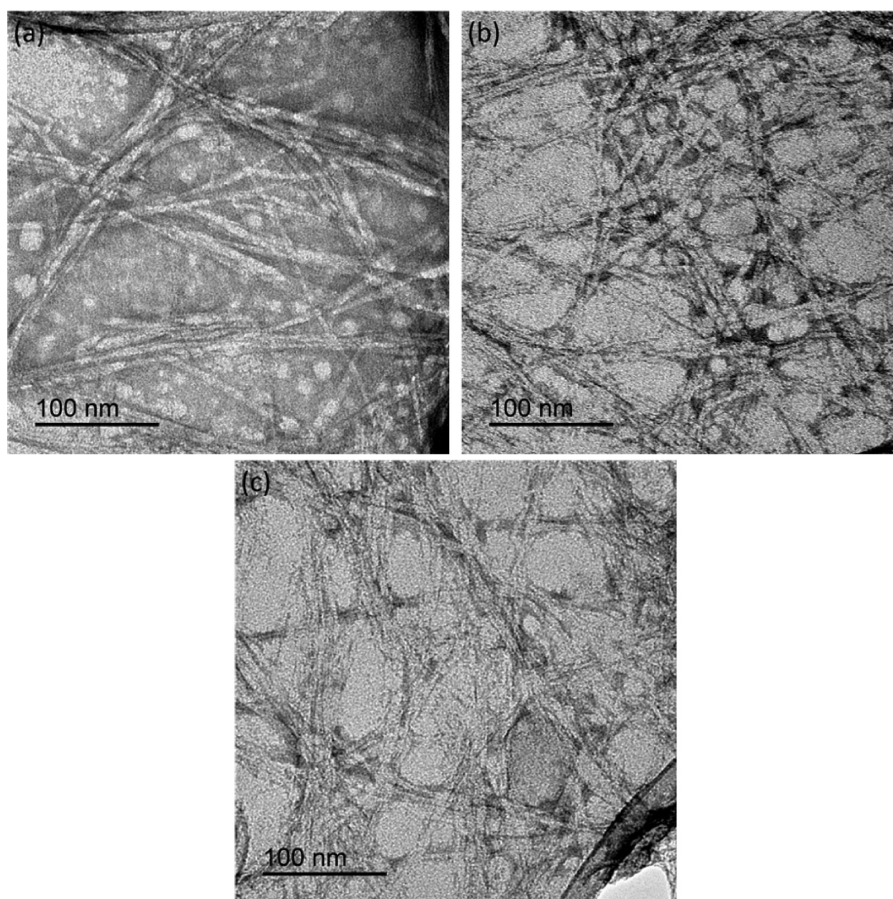


**Figure 8.** Transmission electron microscopy (TEM) images of the nanofibrillated cellulose fiber extracted from microwave liquefied bamboo residues; (a) 120 °C/2%, ultrasonic time, 25 min; (b) 140 °C/25%, ultrasonic time, 5 min; (c) 140 °C/45%, ultrasonic time, 25 min.

## ■ AUTHOR INFORMATION

## Corresponding Author

\*Tingxing Hu. E-mail: [tingxing\\_hu@163.com](mailto:tingxing_hu@163.com). Tel: +86 028-86291456.

## Author Contributions

<sup>†</sup>These authors equally contributed to the work. All authors have given approval to the final version of the paper.

## Funding

This work has been supported by “Key Laboratory of Wood Industry and Furniture Engineering of Sichuan Provincial Colleges and Universities”.

## Notes

The authors declare no competing financial interest.

## ■ ACKNOWLEDGMENTS

This work has been supported by “Key Laboratory of Wood Industry and Furniture Engineering of Sichuan Provincial Colleges and Universities”.

## ■ REFERENCES

- (1) Perlack, R. D.; Stokes, B. J. *Billion-Ton Update: Biomass supply for a bioenergy and bioproducts industry*; Oak Ridge National Laboratory: Oak Ridge, TN, 2011.
- (2) Hakola, M.; Kallioinen, A.; Leskela, M.; Repo, T. From hazardous waste to valuable raw materials: hydrolysis of CCA-treated wood for the production of chemicals. *ChemSusChem* **2013**, *6*, 813–815.
- (3) Song, K. L.; Wu, Q. L.; Zhang, Z.; Ren, S. X.; Lei, T. Z.; Negulescu, I. I.; Zhang, Q. G. Porous carbon nanofibers from electrospun biomass tar/polyacrylonitrile/silver hybrids as antimicrobial materials. *ACS Appl. Mater. Interfaces* **2015**, *7*, 15108–15116.
- (4) Katahira, R.; Mittal, A.; McKinney, K.; Ciesielski, P. N.; Donohoe, B. S.; Black, S. K.; Johnson, D. K.; Bidy, M. J.; Beckham, G. T. Evaluation of clean fractionation pretreatment for the production of renewable fuels and chemicals from corn stover. *ACS Sustainable Chem. Eng.* **2014**, *2*, 1364–1376.
- (5) Zhu, J. Y.; Sabo, R.; Luo, X. L. Integrated production of nanofibrillated cellulose and cellulosic biofuels (ethanol) by enzymatic fractionation of wood fibers. *Green Chem.* **2011**, *13*, 1339–1344.
- (6) Kaldstrom, M.; Meine, N.; Fares, C.; Rinaldi, R.; Schuth, F. Fractionation of ‘water-soluble lignocellulose’ into C5/C6 sugars and sulfur-free lignins. *Green Chem.* **2014**, *16*, 2454–2462.
- (7) Kumar, S.; Lange, J. P.; Rossum, G. V.; Kersten, S. R. A. Liquefaction of lignocellulose in fractionated light bio-oil: proof of concept and techno-economic assessment. *ACS Sustainable Chem. Eng.* **2015**, *3* (9), 2271–2280.
- (8) Li, R. D.; Xie, Y. H.; Yang, T. H.; Li, B. S.; Wang, W. D.; Kai, X. P. Effects of chemical-biological pretreatment of corn stalks on the bio-oils produced by hydrothermal liquefaction. *Energy Convers. Manage.* **2015**, *93*, 23–30.
- (9) Xu, J. M.; Xie, X. F.; Wang, J. X.; Jiang, J. C. Directional liquefaction coupling fractionation of lignocellulosic biomass for platform chemicals. *Green Chem.* **2016**, DOI: [10.1039/C5SGC03070F](https://doi.org/10.1039/C5SGC03070F).
- (10) Hu, S. J.; Wan, C. X.; Li, Y. B. Production and characterization of biopolyols and polyurethane foams from crude glycerol based liquefaction of soybean straw. *Bioresour. Technol.* **2012**, *103*, 227–233.
- (11) Wang, Z.; Xu, S.; Hu, W. P.; Xie, Y. J. Fractionation of the biopolyols from lignocellulosic biomass for the production of rigid foams. *BioEnergy Res.* **2013**, *6*, 896–902.
- (12) Roslan, R.; Zakaria, S.; Chia, C. H.; Boehm, R.; Laborie, M. P. Physico-mechanical properties of resol phenolic adhesives derived from liquefaction of oil palm empty fruit bunch fibres. *Ind. Crops Prod.* **2014**, *62*, 119–124.
- (13) D’Souza, J.; Yan, N. Producing bark-based polyols through liquefaction: effect of liquefaction temperature. *ACS Sustainable Chem. Eng.* **2013**, *1*, 534–540.
- (14) Xu, J. M.; Jiang, J. C.; Hse, C. Y.; Shupe, T. F. Renewable chemical feedstocks from integrated liquefaction processing of lignocellulosic materials using microwave energy. *Green Chem.* **2012**, *14*, 2821–2830.
- (15) Kunaver, M.; Krzan, A. Microwave heating in wood liquefaction. *J. Appl. Polym. Sci.* **2006**, *101*, 1051–1056.
- (16) Zagar, E.; Krzan, A. Microwave driven wood liquefaction with glycols. *Bioresour. Technol.* **2009**, *100*, 3143–3146.
- (17) Pan, H.; Zheng, Z. F.; Hse, C. Y. Microwave-assisted liquefaction of wood with polyhydric alcohols and its application in preparation of polyurethane (PU) foams. *Eur. J. Wood Prod.* **2012**, *70*, 461–470.
- (18) Ouyang, X. P.; Zhu, G. D.; Huang, X. Z.; Qiu, X. Q. Microwave assisted liquefaction of wheat straw alkali lignin for the production of monophenolic compounds. *J. Energy Chem.* **2015**, *24*, 72–76.
- (19) Xie, J. L.; Hse, C. Y.; Shupe, T. F.; Qi, J. Q.; Pan, H. Liquefaction behaviors of bamboo residues in glycerol-based solvent using microwave energy. *J. Appl. Polym. Sci.* **2014**, *131*, DOI: [10.1002/app.40207](https://doi.org/10.1002/app.40207).
- (20) Xie, J. L.; Hse, C. Y.; Shupe, T. F.; Hu, T. X. Influence of solvent type on microwave-assisted liquefaction of bamboo. *Eur. J. Wood Prod.* **2016**, *74*, 249–254.
- (21) Xie, J. L.; Zhai, X. L.; Hse, C. Y.; Shupe, T. F.; Pan, H. Polyols from microwave liquefied bagasse and its application to rigid polyurethane foam. *Materials* **2015**, *8*, 8496–8509.
- (22) Xiao, W. H.; Han, L. J.; Zhao, Y. Y. Comparative study of conventional and microwave-assisted liquefaction of corn stover in ethylene glycol. *Ind. Crops Prod.* **2011**, *34*, 1602–1606.
- (23) Pan, H.; Shupe, T. F.; Hse, C. Y. Characterization of liquefied wood residues from different liquefaction conditions. *J. Appl. Polym. Sci.* **2007**, *105*, 3740–3746.
- (24) Zhang, H. R.; Pang, H.; Shi, J. Z.; Fu, T. Z.; Liao, B. Investigation of liquefied wood residues based on cellulose, hemicellulose, and lignin. *J. Appl. Polym. Sci.* **2012**, *123*, 850–856.
- (25) Jiang, Z. H.; Liu, Z. J.; Fei, B. H.; Cai, Z. Y.; Yu, Y.; Liu, X. The pyrolysis characteristics of moso bamboo. *J. Anal. Appl. Pyrolysis* **2012**, *94*, 48–52.
- (26) Sluiter, A.; Hames, B.; Ruiz, R.; Scarlata, C.; Sluiter, J.; Templeton, D.; Crocker, D. *Determination of Structural Carbohydrates and Lignin in Biomass*; Laboratory Analytical Procedure; NREL/TP-510-42618; National Renewable Energy Laboratory: Golden, CO, 2008; pp 80401–83393.
- (27) Brett, C.; Waldron, K. *Physiology and Biochemistry of Plant Cell Wall*; Springer: London, 1996.
- (28) Khalil, H. P. S. A.; Davoudpour, Y.; Islam, M. N.; Mustapha, A.; Sudesh, K.; Dungani, R.; Jawaid, M. Producing and modification of nanofibrillated cellulose using various mechanical processes: A review. *Carbohydr. Polym.* **2014**, *99*, 649–665.
- (29) Xie, J. L.; Huang, X. Y.; Qi, J. Q.; Hse, C. Y.; Shupe, T. F. Effect of anatomical characteristics and chemical components on microwave-assisted liquefaction of bamboo wastes. *BioResources* **2014**, *9*, 231–240.
- (30) Lin, L. Z.; Yao, Y.; Shiraishi, N. Liquefaction mechanism of  $\beta$ -O-4 lignin model compound in the presence of phenol under acid catalysis. Part I. Identification of the reaction Products. *Holzforchung* **2005**, *55*, 617–624.
- (31) Chen, W. S.; Yu, H. P.; Liu, Y. X.; Hai, Y. F.; Zhang, M. X.; Chen, P. Isolation and characterization of cellulose nanofibers from four plant cellulose fibers using a chemical-ultrasonic process. *Cellulose* **2011**, *18*, 433–442.
- (32) Chirayil, C. J.; Joy, J.; Mathew, L.; Mozetic, M.; Koetz, J.; Thomas, S. Isolation and characterization of cellulose nanofibrils from *Helicteres isora* plant. *Ind. Crops Prod.* **2014**, *59*, 27–34.
- (33) Fahma, F.; Iwamoto, S.; Hori, N.; Iwata, T.; Takemura, A. Isolation, preparation, and characterization of nanofibers from oil palm empty-fruit-bunch (OPEFB). *Cellulose* **2010**, *17*, 977–985.